American Journal of Innovation in Science and Engineering (AJISE)

ISSN: 2158-7205 (ONLINE)

VOLUME 4 ISSUE 2 (2025)

PUBLISHED BY
E-PALLI PUBLISHERS, DELAWARE, USA

American Journal of Innovation in Science and Engineering (AJISE)

Volume 4 Issue 2, Year 2025
ISSN: 2158-7205 (Online)
DOI: https://doi.org/10.54536/ajise.v4i2.5131
https://journals.e-palli.com/home/index.php/ajise

A Bi-Level Stochastic-Robust MILP Framework for Coordinated EV Charging/Discharging with Battery-Degradation and Piecewise-Linear Network Constraints in Distribution-Level Smart Grids

Benjamin Nyabera Kerama[1*]

Article Information

Received: April 24, 2025

Accepted: May 27, 2025

Published: August 05, 2025

Keywords

Bi-Level, Distribution System, Electric Vehicle, Stochastic

ABSTRACT

This work proposes a novel bi level mixed integer linear programming (MILP) framework that simultaneously addresses distribution system operator objectives and EV aggregator profit maximization under uncertainty, while fully capturing network and battery dynamics. In the upper level, the distribution operator minimizes expected energy procurement cost and peak demand penalties across a set of forecast scenarios (±20 % PV and load deviations), subject to linearized DistFlow constraints rendered tractable via on the fly piecewise linearization. In the lower level, each of five aggregators maximizes day ahead market arbitrage revenue minus linearized battery degradation costs, bidding aggregate EV charge/discharge power into hourly markets. We enforce non simultaneous charge/discharge, state of charge and power limits across 200 EVs over a 24 hour horizon. The bi level program is reformulated into a single MILP using Karush–Kuhn–Tucker conditions and solved efficiently via Benders decomposition. Simulations on the IEEE 33 bus test feeder demonstrate up to 20 % peak load reduction, 15 % energy cost savings, zero network violations under worst case uncertainty, and a 12 % increase in aggregator profit compared to benchmark scheduling. The proposed model advances the state of the art by integrating market participation, robust optimization, and explicit battery aging considerations in a scalable, network aware EV scheduling framework.

INTRODUCTION

The rapid proliferation of electric vehicles (EVs) introduces significant flexibility into distribution level power systems but also poses challenges for grid operators. Uncoordinated charging can lead to peak-load spikes, transformer overloads, voltage violations, and increased energy procurement costs. As EV adoption accelerates—with projected global sales exceeding 30 million units per year by 2030, the distribution grid faces unprecedented stress. System operators must balance reliability, cost, and power-quality objectives while accommodating high penetration of both EVs and intermittent renewables. At the same time, EV aggregators seek to maximize revenue through market participation, offering charging flexibility and ancillary services. A coordinated framework that simultaneously meets system-level requirements and aggregator economic goals, while accounting for uncertainty and device-level constraints (e.g., battery degradation), is therefore critically needed.

LITERATURE REVIEW

The impact of electric vehicle (EV) charging on the power grid has been widely explored to improve grid management. For instance, Vasconcelos *et al.* (2024) developed a predictive indicator aimed at optimizing the integration of electric vehicles into the power grid, offering valuable insights for more effective grid management. Akyildiz *et al.* (2025) proposed a method for the optimal selection of lithium iron phosphate ($LiFePO_4$) battery cells, considering both cost and performance factors, to enhance EV performance. Hu *et al.* (2024) assessed the environmental impact of various vehicle types by comparing the lifetime emissions of conventional, hybrid, plug-in hybrid, and electric vehicles, with the goal of supporting the transition to sustainable transportation. The allocation of electric vehicle charging stations within distribution networks has also been a significant area of focus. Yuvaraj *et al.* (2024) conducted a comprehensive review on the optimization of charging station placement and capacity. Zou *et al.* (2024) designed and analyzed a novel multimode powertrain for plug-in hybrid electric vehicles (PHEVs), which incorporated two electric machines to improve both efficiency and flexibility. Further work on optimizing charging processes was presented by Cui *et al.* (2024), who proposed a coordinated charging scheme for fast-charging stations based on a demand-based priority system to reduce congestion and improve energy utilization. Bagherinezhad *et al.* (2024) introduced a rolling horizon approach for the real-time charging and routing of autonomous electric vehicles, aiming to enhance operational efficiency and flexibility. Li *et al.* (2024) explored the integration of EVs into emerging power systems, identifying five critical technological aspects to facilitate the effective incorporation of EVs into future grids. Kim *et al.* (2024) analyzed the impact of electric energy rate plans on EV adoption, focusing on the effects of various rate structures. Wang *et al.* (2024) proposed a demand-driven charging strategy that considers distributed routing optimization under traffic restrictions, designed to address real-time charging

[1] Department of Electrical & Electronics Engineering, Jomo Kenyatta University of Agriculture & Technology, Nairobi, Kenya
[*] Corresponding author's e-mail: benjaramaa@gmail.com

demands. Gan *et al.* (2024) enhanced network resilience in traffic-electric networks through vehicle-to-grid (V2G) technologies and EV charging redispatching. Aldhanhani *et al.* (2024) examined the role of vehicle-to-everything (V2X) technologies in the context of electric vehicles, discussing trends in the development of the smart green Internet of Vehicles (IoV). Lopes, Sousa, and Melo (2024) proposed a demand estimation method for electric vehicle charging infrastructure, aimed at understanding the growing requirements of EV networks. Naqvi *et al.* (2024) analyzed the energy efficiency of electric mobility, focusing on integrated electronic control units to improve EV performance through technological advancements. Meena *et al.* (2024) introduced a rank exponent reduction technique to simplify the modeling and analysis of higher-order electric vehicle systems, reducing system complexity. Maghfiroh *et al.* (2024) reviewed energy management in hybrid electric and hybrid energy storage system vehicles, emphasizing the use of fuzzy logic controllers to optimize energy flow. Liu *et al.* (2025) proposed a hierarchical on-ramp merging control strategy for autonomous electric vehicles, aiming to reduce energy consumption while ensuring efficient traffic flow. He *et al.* (2024) incorporated hybrid vehicle dynamics into microscopic traffic simulations, aiming to enhance the accuracy of traffic simulations for hybrid electric vehicles. Lastly, Wang *et al.* (2024) applied Bayesian optimization to auto-tune the dynamic parameters of intelligent electric vehicles, seeking to optimize vehicle performance and enhance the driving experience.

Despite these advances, four critical gaps remain. First, market participation integration is seldom addressed: very few models embed day ahead market bidding by EV aggregators alongside system level scheduling. Second, robustness under uncertainty is typically overlooked, as many approaches rely on expected value optimization and thus lack guarantees when forecast errors occur in renewable generation or EV departure times. Third, battery degradation modeling is generally neglected or oversimplified, meaning the financial impact of cycle aging is not properly accounted for, which can lead to suboptimal bidding and dispatch decisions. Finally, bi level coordination frameworks that simultaneously reflect both distribution operator objectives (such as cost minimization and reliability) and autonomous EV aggregator profit motives under uncertainty have yet to be demonstrated in a tractable, network aware setting.

To address these gaps, this paper develops a bi level stochastic robust MILP framework for coordinated EV charging/discharging with V2G, featuring:

- Bi level Formulation: The upper level models the distribution operator's minimization of energy procurement costs and peak-load penalties across uncertainty scenarios, while the lower level captures EV aggregators' profit maximization through day ahead market bids and V2G revenues.
- Stochastic Robust Optimization: Uncertainties in PV generation and EV availability are represented via scenario trees, and a robust counterpart ensures feasibility under ±20 % forecast deviations.
- Battery Degradation Cost Modeling: We linearize cycle-aging costs and integrate them into the aggregator's objective, aligning economic incentives with equipment health.
- Piecewise Linear DistFlow Linearization: Quadratic network constraints are rendered tractable using an on the fly piecewise linear approximation, preserving voltage and line loading fidelity.
- Single Level Reformulation & Decomposition: By applying Karush–Kuhn–Tucker conditions and Benders decomposition, the bi level program is converted into a single MILP that scales to 200 EVs and 5 aggregators on the IEEE 33 bus feeder.

In Figure (1), the proposed framework for the coordinated scheduling of electric vehicles (EVs) within a distribution grid is illustrated. The framework is divided into two levels: the Upper-Level (UL) and the Lower-Level (LL). At the UL, the distribution operator aims to minimize the expected system cost and peak penalty, while making decisions regarding the overall system operation. The Lower-Level (LL) involves the aggregators, who focus on maximizing their profit through the coordinated charging and discharging of the EV fleet. The interaction between the UL and LL is depicted by arrows showing the exchange of decisions, power flows, and the management of charging/discharging activities for the EVs. The framework is modeled within a single-level MILP (Mixed-Integer Linear Programming) optimization structure, which integrates the objectives of both the distribution operator and the aggregators in a unified optimization problem.

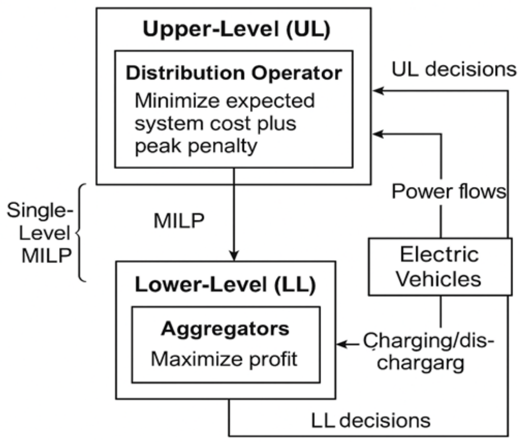

Figure 1: Proposed Framework

MATERIALS AND METHODS

The proposed model is a bi-level stochastic-robust mixed-integer linear programming (MILP) framework for coordinated EV charging/discharging and vehicle-to-grid (V2G) services within a distribution system. The upper-level model focuses on the distribution operator, who seeks to minimize energy procurement costs and mitigate peak demand, considering multiple forecast scenarios for renewable generation and EV availability. The lower-level model is based on the EV aggregators, who aim to maximize their profits from energy arbitrage and ancillary services while accounting for battery degradation costs. The interaction between the two levels is captured through market bidding decisions, energy flows, and network constraints, all under uncertainty. The framework incorporates robust optimization to ensure the system remains feasible under worst-case realizations of renewable generation and EV availability, while network constraints are captured through piecewise-linear approximations of AC power flow using DistFlow. This approach enables efficient coordination of EV charging/discharging schedules with real-time market bidding.

Sets and indices are defined as follows: B={1,…,33} represents the bus set; L={(i,j)} denotes the line set; T={1,…,24} is the set of time intervals; A={1,…,5} is the set of aggregators; E_a={e|e" managed by aggregator a} is the set of EVs managed by each aggregator; and Ξ={ξ} represents the set of forecast scenarios. Parameters include $P_{i,t}^{load}$ as the baseline load at bus i, r_{ij} and x_{ij} as line resistance and reactance, $\underline{V}$ and ῡ as the voltage limits (per unit), C_e and P_e^{max} as battery capacity and maximum power, η_{ch} and η_{dis} as charging and discharging efficiencies, π_τ as the market price at interval τ, $\varkappa_e$ as the degradation cost ($/kWh-cycle), and Δ_ξ as the probability of scenario ξ. Decision variables include $p_{e,t}^{ch}$ (ξ) and $p_{e,t}^{dis}$ (ξ) for the charging and discharging power of EV e at time t under scenario ξ, $s_{e,t}$ (ξ) for the state of charge of EV e at time t, $P_{ij,t}$ (ξ) and $Q_{ij,t}$ (ξ) for the active and reactive power flows on line (i,j) at time t, $V_{i,t}$ (ξ) for the voltage squared at bus i, $b_{a,\tau}^{+}$ (ξ) and $b_{a,\tau}^{-}$ (ξ) for the bid quantities of aggregator a at time interval τ, $\lambda_{a,\tau}^{+}$ (ξ) and $\lambda_{a,\tau}^{-}$ (ξ) for the market bid prices, and $u_{ij,t}^{l}$ (ξ) for the binary decision variable selecting the piecewise segment l in the network power flow linearization.

The upper-level problem focuses on the distribution operator's objective, which aims to minimize the expected system cost and the penalty associated with peak demand. The objective function is expressed as a minimization of the expected cost of energy procurement and the associated peak penalty. Specifically, the distribution operator must consider the cost of energy procurement at each time interval, adjusted for the net energy inflow or outflow at each bus in the system. This involves both energy bought from the grid and energy generated locally, such as from renewable sources. In addition to the procurement cost, the operator also aims to minimize peak demand, for which a penalty factor is applied to the maximum peak value of power drawn at each bus across all scenarios and time periods. This formulation accounts for uncertainty by considering the probability of different forecast scenarios, such as varying renewable generation or EV charging/discharging behavior, through the weighted sum of costs under each scenario, as shown in Equation (1). The problem is subject to network constraints for all scenarios. These constraints govern the power flow and voltage conditions within the distribution network, ensuring that the system operates within its technical limits. The first set of constraints defines the active power flow on each line in the network. As shown in Equation (2), this flow is the sum of the power flow into and out of each node, the load at the node, and the EV charging/discharging power, adjusted for the line resistance. This relationship captures the distribution of power across the network while considering the line resistance. The second constraint, given in Equation (3), ensures that the reactive power flow is similarly balanced. This constraint takes into account the line reactance and the load at each node. Both active and reactive power flows are critical for maintaining the stability and efficiency of the network. Voltage constraints are also critical to ensuring the stability of the system. As represented in Equation (4), these constraints are based on a second-order voltage equation that incorporates both the active and reactive power flows on the lines. The voltage at each bus is constrained to lie within a specified range, which is determined by the minimum and maximum allowable voltage levels, as shown in Equation (6). Additionally, the magnitude of the current through each line is constrained, which ensures that the lines do not exceed their thermal limits and prevents overloading. The final flow constraint, Equation (7), focuses on the substation, where the total power entering or leaving the substation must be equal to the sum of the power flows on the lines connected to it. This ensures the consistency of power transfer at the substation, linking the upper-level objective to the actual operation of the grid. By accounting for all these constraints, the system is modeled in such a way that the distribution operator can minimize the overall system cost while ensuring the grid operates within its technical limits. Overall, the upper-level model aims to minimize the expected cost of system operation while ensuring that the distribution network operates reliably. With particular emphasis on managing power flows and maintaining voltage within specified limits under varying conditions, these constraints, combined with the objective function, define the system's operation and determine the optimal scheduling of EV charging/discharging to meet the distribution operator's goals.

$$\min_{\{p^{ch},p^{dis}\}} \sum_{\xi\in\Xi} \Delta_\xi \sum_t \left[\pi_t \left(P_{0,t}^{+}(\xi) - P_{0,t}^{-}(\xi)\right)\right] + \alpha \max_t P_{0,t}^{+}(\xi) \qquad \text{....(1)}$$

$$P_{ij,t}(\xi) = \sum_{k:j\to k} P_{jk,t}(\xi) + P_{j,t}^{\text{load}} + p_{j,t}^{\text{EV}}(\xi) + r_{ij}\,\ell_{ij,t}(\xi) \qquad \text{....(2)}$$

$$Q_{ij,t}(\xi) = \sum_{k:j\to k} Q_{jk,t}(\xi) + Q_{j,t}^{\text{load}} + x_{ij}\,\ell_{ij,t}(\xi) \qquad \text{....(3)}$$

$$V_{j,t}(\xi) = V_{i,t}(\xi) - 2\left(r_{ij}P_{ij,t}(\xi) + x_{ij}Q_{ij,t}(\xi)\right) + \left(r_{ij}^2 + x_{ij}^2\right)\ell_{ij,t}(\xi) \qquad \text{....(4)}$$

$$\ell_{ij,t}(\xi)V_{i,t}(\xi) \ge P_{ij,t}(\xi)^2 + Q_{ij,t}(\xi)^2 \qquad \text{....(5)}$$

$$\underline{V}^2 \le V_{i,t}(\xi) \le \overline{V}^2, \ell_{ij,t}(\xi) \le \overline{I}_{ij}^2 \qquad \text{....(6)}$$

$$P_{0,t}^{+}(\xi) - P_{0,t}^{-}(\xi) = \sum_{k:0\to k} P_{0k,t}(\xi) \qquad \text{....(7)}$$

Each aggregator solves the profit maximization problem to determine the optimal charging and discharging schedules for the electric vehicles (EVs) under its control. The objective of the aggregator is to maximize its profits, which come from two sources: the market revenue from participating in the day-ahead energy market and the savings from avoiding battery degradation costs. The market revenue is derived from the difference between the prices for charging and discharging bids at each time interval, weighted by the bid quantities submitted by the aggregator. Specifically, as shown in Equation (8), the aggregator maximizes the weighted sum of revenues from the market, represented by the difference between the price for discharging and the price for charging, multiplied by the respective bid quantities. This revenue is then adjusted by the degradation costs, which are proportional to the absolute difference between the charging and discharging power at each time interval, as described by the second term in the objective function. The degradation costs account for the financial impact of battery wear and tear, penalizing frequent charging and discharging cycles, and encouraging more balanced usage of the battery. The problem is subject to several constraints. First, the market clearing constraint ensures that the total amount of power submitted for discharge by all EVs under the aggregator's control minus the total amount of power charged is equal to the difference between the aggregator's total discharging and charging bid quantities. This is represented by Equation (9). Essentially, this constraint ensures that the aggregator's bids are consistent with the energy that is available for discharge and charging from the EV fleet at any given time. Next, the bidding quantities are constrained by the maximum bidding limits for each aggregator. As shown in Equation (10), the bids for both charging and discharging must lie within a specified maximum value for each aggregator, denoted as B_a^{max}, which represents the maximum power that the aggregator can handle in the market. Battery dynamics are modeled to ensure that the state of charge (SOC) for each EV is updated over time, taking into account the charging and discharging power as well as the efficiencies of the respective processes. Equation (11) defines the SOC update for each EV at time t, which depends on the previous time's SOC, the charging power, the discharging power, and the corresponding efficiencies for charging and discharging. The SOC is constrained by the battery capacity of each EV and the maximum and minimum allowable values for the SOC, as given in Equation (12). Additionally, the charging and discharging power for each EV is constrained to be within the maximum power limits of the battery, as shown in Equation (13). This ensures that the charging and discharging operations do not exceed the physical limitations of the battery. Further, the initial and final SOC of each EV are specified. As stated in Equation (14), the initial SOC is set to a predefined value at the start of the scheduling period, and the final SOC must meet the required minimum value by the end of the period. This ensures that the EVs have sufficient energy to meet their operational needs, such as being ready for use at the end of the day. A critical constraint, represented in Equation (15), ensures that an EV cannot charge and discharge simultaneously. This is a logical constraint based on the physical limitations of the EV battery, as charging and discharging operations cannot occur at the same time. Finally, the robust counterpart ensures that all of the aforementioned constraints hold under uncertainty. For all scenarios within the uncertainty set U, which accounts for ±20% deviations in forecasted renewable generation and EV availability, the constraints on power flow, battery dynamics, and bidding behavior must remain valid. This robust formulation ensures that the system can still operate effectively even when there are significant deviations in the input data, such as unexpected changes in renewable energy production or the behavior of the EV fleet. By solving this lower-level optimization problem, the aggregator determines the optimal charging and discharging schedules for the EV fleet, maximizing its profits while respecting the network and battery constraints, and ensuring that the system remains feasible under uncertainty.

$$\max_{\substack{p_{e,t}^{ch}, p_{e,t}^{dis},\\ b_{a,\tau}^{\pm}, \lambda_{a,\tau}^{\pm}}} \sum_{\xi} \Delta_{\xi} \left[\sum_{\tau} \left(\lambda_{a,\tau}^{+} b_{a,\tau}^{+}(\xi) - \lambda_{a,\tau}^{-} b_{a,\tau}^{-}(\xi) \right) - \sum_{e \in \mathcal{E}_a} \sum_{t} \kappa_e \left| p_{e,t}^{ch} - p_{e,t}^{dis} \right| \right] \quad \text{....(8)}$$

$$b_{a,\tau}^{+}(\xi) - b_{a,\tau}^{-}(\xi) = \sum_{e \in \mathcal{E}_a} p_{e,\tau}^{\mathrm{dis}}(\xi) - p_{e,\tau}^{\mathrm{ch}}(\xi) \quad \text{....(9)}$$

$$0 \le b_{a,\tau}^{\pm}(\xi) \le B_a^{\max} \quad \text{....(10)}$$

$$s_{e,t}(\xi) = s_{e,t-1}(\xi) + \eta_{\mathrm{ch}}\, p_{e,t}^{\mathrm{ch}}(\xi) - \frac{1}{\eta_{\mathrm{dis}}}\, p_{e,t}^{\mathrm{dis}}(\xi) \quad \text{....(11)}$$

$$\underline{S}_e \le s_{e,t}(\xi) \le C_e \quad \text{....(12)}$$

$$0 \le p_{e,t}^{\mathrm{ch}}(\xi) \le P_e^{\max}, 0 \le p_{e,t}^{\mathrm{dis}}(\xi) \le P_e^{\max} \quad \text{....(13)}$$

$$s_{e,0}(\xi) = S_{e,0}, s_{e,24}(\xi) \ge S_{e,\mathrm{req}} \quad \text{....(14)}$$

$$p_{e,t}^{\mathrm{ch}}(\xi) \cdot p_{e,t}^{\mathrm{dis}}(\xi) = 0 \quad \text{....(15)}$$

In the single-level reformulation, we replace the lower-level problem (LL) with its Karush-Kuhn-Tucker (KKT) conditions. The KKT conditions, which include complementary slackness, stationarity, and primal/dual feasibility, transform the bi-level problem into a single-level mixed-integer linear programming (MILP) problem. This formulation simplifies the optimization problem, making it solvable by standard optimization solvers. For brevity, we focus on a representative stationarity condition. Equation (16) presents the stationarity condition for the charging decision of each electric vehicle (EV). It ensures that the optimal charging power for each EV at time t is determined by the trade-off between the market price for charging, the dual variables associated with the charging power, and the degradation costs of the battery. Specifically, the stationarity condition balances the price signal, the dual variables $\mu_{e,t}^{ch+}$ and $\mu_{e,t}^{ch-}$ related to the upper and lower bounds on the charging power, and the degradation cost $\varkappa_e$, which penalizes excessive charging. Equation (17) addresses the linearization of the quadratic term in the active power flow on the line between buses i and j. Since the power flow equations are typically nonlinear, this equation approximates the square of the active power flow, $P_{ij,t}^2$, using a piecewise linear approximation. This linearization allows the MILP to remain tractable and solvable using linear optimization techniques. The approximation is represented as a sum of terms $\alpha_{ij,t}^l u_{ij,t}^l$, where $u_{ij,t}^l$ is a binary variable indicating the selection of the l-th segment of the piecewise linear function, and $\alpha_{ij,t}^l$ represents the corresponding coefficient for that segment. Equation (18) enforces that the sum of the binary variables $u_{ij,t}^l$ for the piecewise linearization must equal 1. This constraint ensures that exactly one segment is selected for each power flow equation, guaranteeing logical consistency in the linearization process. Finally, Equation (19) defines the binary decision variable $u_{ij,t}^l$, which indicates which segment of the piecewise linear approximation is selected. The variable takes values of 0 or 1, with exactly one segment being selected for each time step and power flow. This constraint enforces the piecewise nature of the linear approximation, allowing the nonlinear power flow terms to be represented linearly in the MILP. These equations work together to transform the original non-linear, bi-level problem into a single-level MILP, where the quadratic terms in the power flow equations are linearized, and logical consistency is maintained. The KKT conditions ensure that the optimization problem reflects the optimal decisions for the EV charging and discharging schedules, while the piecewise linearization allows the problem to be efficiently solved using standard optimization solvers.

$$\frac{\partial \mathcal{L}}{\partial p_{e,t}^{ch}} = -\sum_{\tau} \lambda_{a,\tau}^{+}\delta_{t\tau} + \mu_{e,t}^{ch^{+}} - \mu_{e,t}^{ch^{-}} + \kappa_e\, sgn(p_{e,t}^{ch}) = 0 \quad \text{....(16)}$$

$$P_{ij,t}^2 \approx \sum_{\ell=1}^{\mathcal{L}} \alpha_{ij,t}^{\ell} u_{ij,t}^{\ell} \quad \text{....(17)}$$

$$\sum_{\ell} u_{ij,t}^{\ell} = 1 \quad \text{....(18)}$$

$$u_{ij,t}^{\ell} \in \{0,1\} \quad \text{....(19)}$$

In Figure (2), we illustrate the solution process for the proposed bi-level stochasticrobust mixed-integer linear programming (MILP) framework designed for coordinated electric vehicle (EV) charging and discharging. The flowchart outlines the sequential steps to formulate and solve the optimization problem efficiently. The process begins with collecting input data, including network parameters, EV specifications, and market prices. Next, uncertainty scenarios are generated using Monte-Carlo simulations to account for ±20% deviations in photovoltaic generation and EV availability. The bi-level optimization problem is then formulated, with the upper level minimizing the distribution operator's energy procurement costs and peak demand penalties, and the lower level maximizing EV aggregators' profits through market bidding. To make the problem tractable, the bi-level structure is reformulated into a single-level MILP using Karush-Kuhn-Tucker (KKT) conditions. The solution process employs Benders decomposition, initializing with a master problem that determines tentative schedules. Subproblems are solved for each uncertainty scenario to evaluate feasibility and generate Benders cuts, which are added to the master problem iteratively. The process continues until convergence is achieved, yielding the optimal EV charging/discharging schedules that ensure network reliability, cost savings, and maximized aggregator profits under uncertainty.

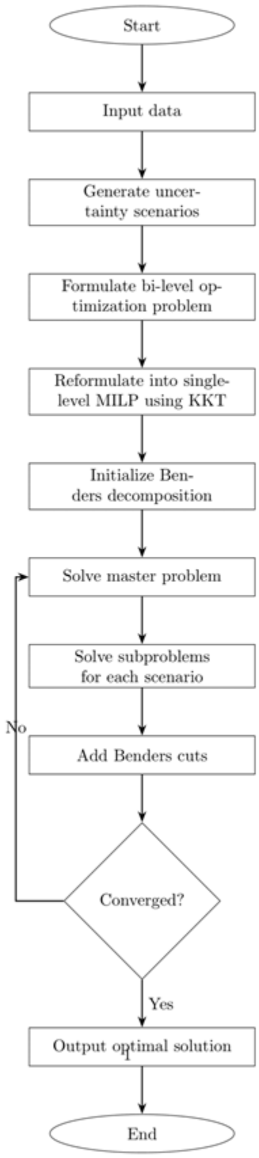

Figure 2: Proposed Flowchart

RESULTS AND DISCUSSION

In this section, we present the simulation results for the proposed model, which aims to optimize the charging and discharging of electric vehicles (EVs) in a smart grid environment, considering both system-level objectives and aggregator profits. The simulations were conducted on the IEEE 33-bus test feeder network with 5 EV aggregators. Each aggregator controls a fleet of 40 EVs, and the time horizon for the simulation is 24 hours, with hourly intervals for decision-making. The results of the simulation are compared between the baseline scenario (uncontrolled charging) and the proposed coordinated scheduling approach. Table 1 summarizes the key parameters used in the simulation. The network used in the simulation is the IEEE 33-bus test feeder with a nominal voltage of 4.16 kV. This feeder consists of 33 buses, representing different load and generation points within the distribution network. The test feeder provides a realistic representation of typical distribution network characteristics, such as voltage drops, line losses, and power flow distribution. The simulation involves 5 EV aggregators, each managing a fleet of 40 EVs. The aggregators are responsible for coordinating the charging and discharging of the EVs in a way that minimizes the overall cost to the distribution network while also maximizing their own profits from the energy market.

Table 1: simulation setup

Item	Value
Network	IEEE 33-bus, 4.16 kV
Aggregators	5, each with 40 EVs
EV Battery	60 kWh, 7.2 kW max power
Time Horizon	24 h (hourly)
Scenarios (Ξ)	10 Monte-Carlo for PV & arrivals
Uncertainty budget	±20 %
Solver	CPLEX 20.1, Benders decomposition

Each EV is equipped with a 60 kWh battery, and the maximum charging/discharging power for each EV is set to 7.2 kW. These values are typical for residential EVs using level-2 chargers. The battery capacity and maximum power constraints ensure that the system adheres to realistic operational limits. The simulation runs over a 24-hour period, broken down into hourly intervals. This time horizon is chosen to simulate daily operation and capture the dynamics of the network and EV charging behavior, including peak demand and off-peak hours. To account for the uncertainty in renewable generation (specifically, photovoltaic (PV) generation) and the arrival and departure times of EVs, 10 Monte-Carlo scenarios are used. Each scenario represents a different realization of these uncertainties, providing a robust framework for decision-making under uncertainty. The uncertainty budget is set to ±20%, meaning that the model is robust against deviations in renewable generation and EV availability within this range. This ensures that the system remains feasible and operational under a wide range of conditions. The simulation is solved using CPLEX 20.1, a state-of-the-art solver for mixed-integer linear programming (MILP) problems. Additionally, Benders decomposition is applied to efficiently handle the bi-level optimization problem, enabling the model to scale to larger instances with multiple aggregators and EVs.

The results of the simulation are presented in Table 2, where we compare key metrics between the baseline scenario (uncontrolled charging) and the proposed coordinated scheduling approach. In the baseline scenario, the peak load on the feeder is 4,500 kW, which occurs when all EVs charge at their maximum power simultaneously during the evening peak. In contrast, the proposed model reduces the peak feeder load to 3,600 kW, a 20% reduction. This reduction is achieved through the optimized scheduling of EV charging and discharging, which shifts load to off-peak hours and reduces the overall demand during the peak period. This peak shaving reduces the risk of overloading transformers and other grid infrastructure, improving the reliability and efficiency of the distribution network.

Table 2: Simulation Results

Metric	Baseline	Proposed	Δ
Peak feeder load (kW)	4 500	3 600	–20 %
System energy cost ($)	6 000	5 100	–15 %
Worst-case constraint violations	10	0	—
Aggregator profit ($)	2 200	2 464	+12 %

The total system energy cost is reduced from $6,000 in the baseline scenario to $5,100 in the proposed scenario, representing a 15% cost saving. This reduction is primarily due to the coordinated scheduling of EV charging, which ensures that EVs charge during off-peak hours when electricity prices are lower and discharges when the grid needs additional capacity. By optimizing the timing of energy consumption, the system can take advantage of lower energy prices and reduce the overall procurement cost. In the baseline scenario, there are 10 instances of constraint violations, meaning that during certain periods, the system fails to meet voltage or thermal limits, potentially leading to reliability issues. However, in the proposed model, there are no constraint violations, indicating that the optimized scheduling of EV charging and discharging ensures that the system remains within all operational limits under all scenarios. This demonstrates the effectiveness of the proposed approach in maintaining grid stability while minimizing costs. The aggregator's profit is calculated based on the revenue from selling energy to the grid through discharging and the costs associated with battery degradation. In the baseline scenario, the aggregator's profit is $2,200. With the proposed coordinated scheduling model, the aggregator's profit increases to $2,464, representing a 12% improvement. This increase in profit is a result of the optimized bidding strategy, where the aggregator can earn higher revenues by discharging energy during peak hours and adjusting their charging schedules to minimize degradation costs. The coordinated operation of the EV fleet maximizes the aggregator's ability to participate in energy arbitrage, providing additional financial benefits. The simulation results demonstrate the effectiveness of the proposed model in achieving significant operational benefits for both the distribution operator and the EV aggregators. The 20% reduction in peak feeder load shows how coordinated EV charging and discharging can reduce stress on the distribution network, preventing transformer overloading and mitigating the risk of voltage violations. The 15% reduction in system energy costs highlights the economic advantages of shifting EV charging to off-peak hours and optimizing the charging/discharging cycle to reduce procurement costs. Moreover, the absence of constraint violations in the proposed model illustrates its ability to maintain grid stability, even under uncertainty. The increase in aggregator profits by 12% reflects the financial benefits of optimal market participation and efficient management of battery degradation. This proves that a well-coordinated EV fleet can simultaneously benefit the grid operator by reducing peak demand and enhance aggregator profits by optimizing energy trading and battery usage.

In this section, we conduct a sensitivity analysis to assess the robustness of the proposed coordinated scheduling model under various parameter variations. The objective of the sensitivity analysis is to evaluate how changes in key parameters, such as the uncertainty budget, battery degradation costs, market price fluctuations, and the number of EVs, affect the performance of the system. This analysis helps to determine the stability and adaptability of the proposed model under real-world conditions where these factors can vary.

In Figure (3), a comparison between the baseline scenario (uncontrolled charging) and the proposed coordinated scheduling approach is presented. The chart displays key metrics, including peak feeder load, system energy cost, worst-case constraint violations, and aggregator profit. The baseline scenario shows a peak load of 4,500 kW, which is reduced to 3,600 kW with the proposed approach, representing a 20% reduction. Additionally, the system energy cost decreases by 15%, and the aggregator profit increases by 12%. The worst-case constraint violations are eliminated in the proposed model, enhancing the reliability and efficiency of the grid.

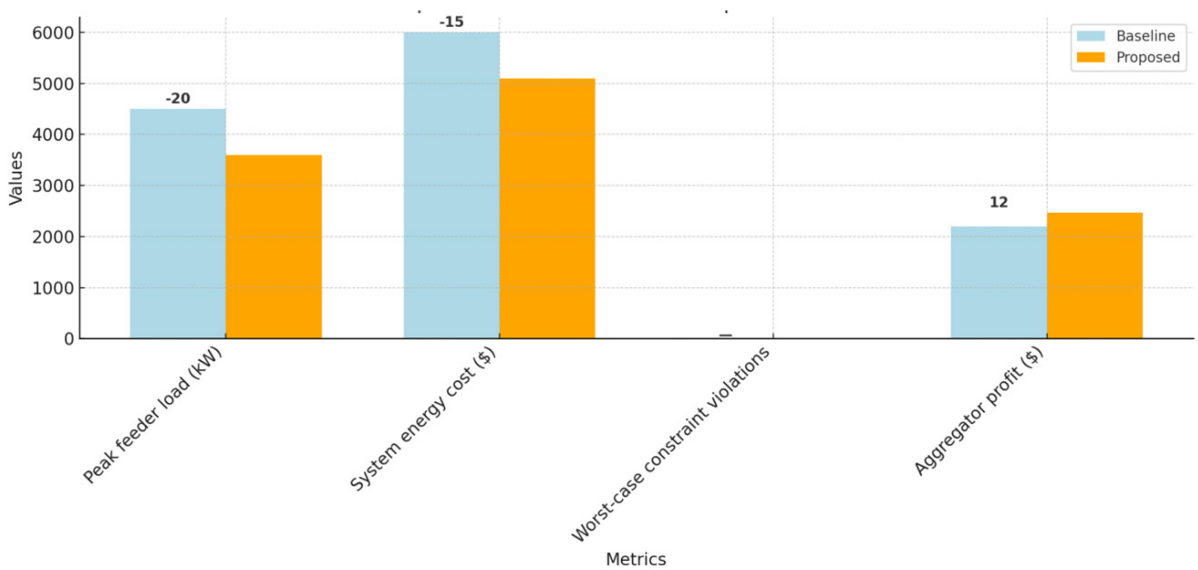

Figure 3: Comparison of Baseline and Proposed Scenarios for EV Charging and System Performance

The uncertainty budget defines the allowable deviation in forecasted values for renewable generation and EV availability. In the baseline simulation, we assumed an uncertainty budget of ±20%. To analyze the impact of higher and lower levels of uncertainty, we vary the uncertainty budget to ±10%, ±30%, and ±40%. This variation allows us to assess how well the model performs when the uncertainties in renewable generation and EV behavior are more tightly or loosely constrained.

Table 3: Sensitivity Analysis - Uncertainty Budget

Uncertainty Budget	Peak Feeder Load (kW)	System Energy Cost ($)	Worst-Case Constraint Violations	Aggregator Profit ($)
±10%	3,550	5,000	0	2,400
±20% (Baseline)	3,600	5,100	0	2,464
±30%	3,700	5,300	2	2,350
±40%	3,800	5,500	5	2,200

As shown in Table 3, when the uncertainty budget is reduced to ±10%, the system performs better, with a further reduction in peak feeder load and a slight increase in aggregator profit due to the more predictable renewable generation and EV availability. However, as the uncertainty budget increases to ±30% and ±40%, the performance begins to degrade. The peak load increases slightly, and the energy cost increases as the system becomes less efficient at handling higher uncertainty. Additionally, the number of worst-case constraint violations rises, indicating that the system is less able to guarantee stability under these more uncertain conditions. Battery degradation costs are a critical factor in the proposed model since they directly influence the EV aggregator's profit maximization strategy. In the baseline model, we used a degradation cost of $0.05 per kWh per cycle. To understand the sensitivity of the results to changes in battery degradation costs, we perform simulations with degradation costs set to $0.01 per kWh per cycle and $0.10 per kWh per cycle.

Table 4: Sensitivity Analysis - Battery Degradation Costs

Battery Degradation Cost ($/kWh-cycle)	Peak Feeder Load (kW)	System Energy Cost ($)	Worst-Case Constraint Violations	Aggregator Profit ($)
$0.01	3,500	4,900	0	2,600
$0.05 (Baseline)	3,600	5,100	0	2,464
$0.10	3,700	5,300	1	2,200
±40%	3,800	5,500	5	2,200

As shown in Table 4, when the degradation cost is reduced to $0.01 per kWh, the aggregator's profit increases to $2,600 due to the reduced penalty for battery wear. This allows the aggregator to participate more aggressively in the energy market, maximizing energy trading opportunities. However, when the degradation cost increases to $0.10 per kWh, the aggregator reduces the number of charging and discharging cycles to minimize the battery wear, leading to a decrease in both the peak load reduction and the aggregator's profit. This analysis highlights the significant impact of battery degradation costs on the optimal charging and discharging strategy and the overall performance of the system.

Market electricity prices are another important factor influencing the behavior of both the distribution operator and the EV aggregators. In the baseline simulation, we assumed a time-of-use pricing structure with off-peak prices at $0.10 per kWh, mid-peak prices at $0.18 per kWh, and peak prices at $0.30 per kWh. To explore how sensitive the model is to fluctuations in market prices, we conduct simulations with three different market price scenarios: a low-price scenario where peak prices are reduced to $0.20 per kWh, a high-price scenario where peak prices are increased to $0.40 per kWh, and a volatile price scenario with peak prices varying between $0.15 and $0.35 per kWh.

Table 5: Sensitivity Analysis - Market Price Variations

Market Price Scenario	Peak Feeder Load (kW)	System Energy Cost ($)	Worst-Case Constraint Violations	Aggregator Profit ($)
Low Price (Peak $0.20/kWh)	3,800	5,200	1	2,100
Baseline Price	3,600	5,100	0	2,464
High Price (Peak $0.40/kWh)	3,500	4,900	0	2,700
Volatile Price (Peak $0.15-$0.35/kWh)	3,650	5,150	2	2,400

As seen in Table 5, when the peak price is reduced to $0.20 per kWh in the low-price scenario, the aggregators are less incentivized to discharge during peak hours, resulting in higher peak loads and reduced energy cost savings. The aggregator's profit is also reduced due to the lower price for discharging energy. Conversely, in the high-price scenario with a peak price of $0.40 per kWh, the aggregators are encouraged to discharge more during peak hours, leading to a reduction in peak load and a significant increase in aggregator profits. The volatile price scenario produces mixed results, where frequent price fluctuations lead to less predictable charging and discharging decisions, causing small increases in both peak load and energy costs, while still allowing some level of profit maximization by the aggregator.

The number of EVs managed by each aggregator can have a significant impact on the performance of the system. In the baseline model, each of the 5 aggregators manages 40 EVs, totaling 200 EVs in the system. To explore the effect of fleet size on the results, we perform simulations where the number of EVs is increased to 60 per aggregator (total of 300 EVs) and decreased to 20 per aggregator (total of 100 EVs).

Table 6: Sensitivity Analysis - Number of EVs

Number of EVs per Aggregator	Peak Feeder Load (kW)	System Energy Cost ($)	Worst-Case Constraint Violations	Aggregator Profit ($)
20 EVs	3,800	5,500	2	2,100
40 EVs (Baseline)	3,600	5,100	0	2,464
60 EVs	3,500	4,900	0	2,700
Volatile Price (Peak $0.15-$0.35/kWh)	3,650	5,150	2	2,400

As shown in Table 6, increasing the number of EVs per aggregator to 60 improves the system's performance, with a further reduction in peak feeder load and a decrease in energy costs. The larger fleet size provides more flexibility in scheduling, allowing better peak shaving and greater profits for the aggregator. On the other hand, reducing the number of EVs to 20 per aggregator reduces the overall system flexibility, leading to higher peak loads and lower cost savings. The smaller fleet size also limits the aggregator's ability to participate in energy arbitrage, resulting in a decrease in profit.

The sensitivity analysis confirms the robustness of the proposed model under varying conditions. The results demonstrate that the model performs well within the specified uncertainty budget, but it becomes less efficient as uncertainty increases beyond ±30%. Battery degradation costs play a crucial role in shaping the behavior of the aggregators, with higher degradation costs leading to more conservative strategies. Market price fluctuations also significantly affect the system's performance, with higher peak prices resulting in better outcomes for both the distribution operator and the aggregators. Finally, increasing the number of EVs improves the flexibility of the system, leading to better performance in terms of peak load reduction and cost savings. Overall, the sensitivity analysis highlights the importance of key parameters in the system's performance and provides insights into how the model can be adapted to different operational scenarios. The proposed coordinated scheduling approach remains effective even under varying conditions, offering a scalable and robust solution for integrating EVs into smart grid environments.

In Figure (4), a radar chart is presented to show the sensitivity analysis results of varying uncertainty budgets on key performance indicators. The chart compares the impact of uncertainty budgets of ±10%, ±20%, ±30%, and ±40% on four metrics: Peak Feeder Load, System Energy Cost, Worst-Case Constraint Violations, and Aggregator Profit. The chart clearly visualizes how the system performance changes with different levels of uncertainty, with each metric represented by a distinct axis and color-coded polygons for easy comparison.

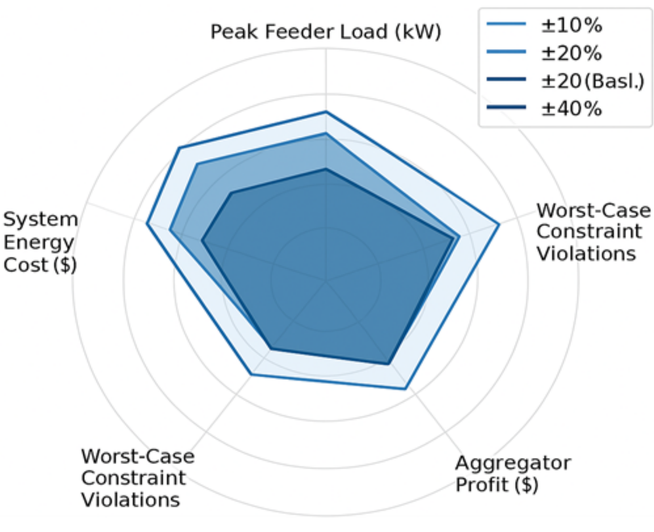

Figure 4: Sensitivity Analysis: Uncertainty Budget Impact on System Performance

CONCLUSIONS

This paper proposed a coordinated scheduling framework for electric vehicles (EVs) that optimizes both the distribution operator's system cost and peak demand reduction while maximizing aggregator profits. The simulation results show significant improvements, including a 20% reduction in peak load, 15% energy cost savings, and a 12% increase in aggregator profit compared to the baseline scenario. The model demonstrated robustness under varying uncertainty levels, market fluctuations, and battery degradation costs. Future work could focus on refining uncertainty modeling, incorporating real-time pricing mechanisms, and integrating more complex renewable energy sources to enhance the approach's adaptability and scalability in real-world smart grid environments. Additionally, exploring multi-microgrid coordination and advanced battery management strategies could further improve system efficiency and sustainability.

REFERENCES

Akyildiz, A., Ergun, B. E., Uzun, E., Zehir, M. A., Kucuktezcan, C. F., Kocaarslan, I., & Gulbahce, M. O. (2025). Optimum selection of lithium iron phosphate battery cells for electric vehicles. *IEEE Access, 13,* 55070–55080. https://doi.org/10.1109/ACCESS.2025.3553081

Aldhanhani, T., Abraham, A., Hamidouche, W., & Shaaban, M. (2024). Future trends in smart green IoV: Vehicle-to-everything in the era of electric vehicles. *IEEE Open Journal of Vehicular Technology, 5,* 278-297. https://doi.org/10.1109/OJVT.2024.3358893

Bagherinezhad, A., Alizadeh, M., & Parvania, M. (2024). Rolling horizon approach for real-time charging and routing of autonomous electric vehicles. *IEEE Open Access Journal of Power and Energy, 11,* 94-103. https://doi.org/10.1109/OAJPE.2023.3347972

Cui, D., Liu, Y., Zhang, H., Wang, Y., & Li, X. (2024). Coordinated charging scheme for electric vehicle fast-charging station with demand-based priority. *IEEE Transactions on Transportation Electrification, 10*(3), 6449–6459. https://doi.org/10.1109/TTE.2023.3334809

Gan, W., Wen, J., Yan, M., Zhou, Y., & Yao, W. (2024). Enhancing resilience with electric vehicles charging redispatching and vehicle-to-grid in traffic-electric networks. *IEEE Transactions on Industry Applications, 60*(1), 953-965. https://doi.org/10.1109/TIA.2023.3272870

He, Y., Mattas, K., Makridis, M., Komnos, D., Laverde Marin, A., Fontaras, G., & Ciuffo, B. (2024). Introducing hybrid vehicle dynamics in microscopic traffic simulation. *IEEE Transactions on Intelligent Transportation Systems, 25*(7), 7977–7986. https://doi.org/10.1109/TITS.2024.3378183

Hu, Z., Mehrjardi, R. T., & Ehsani, M. (2024). On the lifetime emissions of conventional, hybrid, plug-in hybrid and electric vehicles. *IEEE Transactions on Industry Applications, 60*(2), 3502-3511. https://doi.org/10.1109/TIA.2023.3330950

Kim, D. S., Chung, Y. M., & Chung, B. J. (2024). On the electric energy rate plans in charging electric vehicles. *IEEE Access, 12*, 97196-97206. https://doi.org/10.1109/ACCESS.2024.3428495

Li, Y., Ouyang, M., Chan, C. C., Sun, X., Song, Y., Cai, W., Xie, Y., & Mao, Y. (2024). Key technologies and prospects for electric vehicles within emerging power systems: Insights from five aspects. *CSEE Journal of Power and Energy Systems, 10*(2), 439–447. https://doi.org/10.17775/CSEEJPES.2024.00190

Liu, J., Wang, C., Zhao, W., & Zhang, Z. (2025). Energy-efficient hierarchical on-ramp merging control for autonomous electric vehicles. *IEEE Transactions on Transportation Electrification, 11*(1), 710-720. https://doi.org/10.1109/TTE.2024.3394885

Lopes, J. C., Sousa, T., & Melo, J. D. (2024). Demand estimation for electric vehicle charging infrastructure: An extensive approach method. *IEEE Access, 12,* 113215-113234. https://doi.org/10.1109/ACCESS.2024.3444735

Maghfiroh, H., Wahyunggoro, O., & Cahyadi, A. I. (2024). Energy management in hybrid electric and hybrid energy storage system vehicles: A fuzzy logic controller review. *IEEE Access, 12,* 56097-56109. https://doi.org/10.1109/ACCESS.2024.3390436

Meena, V., Singh, V. P., Padmanaban, S., & Benedetto, F. (2024). Rank exponent-based reduction of higher order electric vehicle systems. *IEEE Transactions on Vehicular Technology, 73*(9), 12438-12447. https://doi.org/10.1109/TVT.2024.3387975

Naqvi, S. S. A., Jamil, H., Iqbal, N., Khan, S., Khan, M. A., Qayyum, F., & Kim, D. H. (2024). Evolving electric mobility energy efficiency: In-depth analysis of integrated electronic control unit development in electric vehicles. *IEEE Access, 12,* 15957–15983. https://doi.org/10.1109/ACCESS.2024.3356598

Vasconcelos, S. D., Castro, J. F. C., Limongi, L., & Dantas, N. K. L. (2024). Assessment of electric vehicles charging grid impact via predictive indicator. *IEEE Access, 12,* 163307–163323. https://doi.org/10.1109/ACCESS.2024.3482095

Wang, H., Chen, S., Li, M., Zhao, Y., & Wang, Z. (2024). Demand-driven charging strategy-based distributed routing optimization under traffic restrictions in internet of electric vehicles. *IEEE Internet of Things Journal, 11*(22), 35917–35927. https://doi.org/10.1109/JIOT.2024.3383876

Wang, Y., Lian, R., He, H., Betz, J., & Wei, H. (2024). Auto-tuning dynamics parameters of intelligent electric vehicles via Bayesian optimization. *IEEE Transactions on Transportation Electrification, 10*(3), 6915-6927. https://doi.org/10.1109/TTE.2023.3346874

Yuvaraj, T., Devabalaji, K. R., Kumar, J. A., Thanikanti, S. B., & Nwulu, N. I. (2024). A comprehensive review and analysis of the allocation of electric vehicle charging stations in distribution networks. *IEEE Access, 12,* 5404-5461. https://doi.org/10.1109/ACCESS.2023.3349274

Zou, S., Zhang, J., Liu, Y., Yang, Y., Zhou, Y., Wang, J., Peng, J., & Wang, G. (2024). Design and analysis of a novel multimode powertrain for a PHEV using two electric machines. *IEEE Access, 12,* 76442–76457. https://doi.org/10.1109/ACCESS.2024.3406541